

Review

# The Use of Copper Oxide Thin Films in Gas-Sensing Applications

Artur Rydosz 

Department of Electronics, AGH University of Science and Technology, 30059 Krakow, Poland; artur.rydosz@agh.edu.pl; Tel.: +48-12-617-2594

Received: 15 October 2018; Accepted: 20 November 2018; Published: 26 November 2018



**Abstract:** In this work, the latest achievements in the field of copper oxide thin film gas sensors are presented and discussed. Several methods and deposition techniques are shown with their advantages and disadvantages for commercial applications. Recently, CuO thin film gas sensors have been studied to detect various compounds, such as: nitrogen oxides, carbon oxides, hydrogen sulfide, ammonia, as well as several volatile organic compounds in many different applications, e.g., agriculture. The CuO thin film gas sensors exhibited high 3-S parameters (sensitivity, selectivity, and stability). Furthermore, the possibility to function at room temperature with long-term stability was proven as well, which makes this material very attractive in gas-sensing applications, including exhaled breath analysis.

**Keywords:** gas sensors; nanomaterials; exhaled acetone detection; diabetes

## 1. Introduction

Gas detectors have been continuously developed over the last few decades as a result of increasing industrialization. In 1953, Brattain and Bardeen discovered that gas adsorption onto a semiconductor produces a change in the electrical conductance of its material [1]. The first commercially-available gas sensor was introduced in 1968 by Taguchi for the detection of hydrocarbons [2]. Since then, gas detectors have been used to monitor environmental pollution, domestic safety, public security, automotive applications, air quality, and more recently, to make medical diagnoses, such as exhaled breath analysis. Gas detectors have been fabricated in many different ways, such as: electrochemical and optical approaches, and solid state gas sensors with various gas sensing materials, e.g., metal oxides (MOXs). For such gas sensors, the most widely-accepted sensing mechanism can be explained by the resistance change, which is caused by the surface reaction upon exposure to different gaseous atmospheres, and this is related to their composition, crystalline size, and structure. Over the last 60 years, the gas sensing mechanisms have been studied in terms of various materials (n-type, p-type), several measurement techniques, such as: static and dynamic thermal modulation, doping effects, micro- and nano-structures, etc. CuO is the most widely-studied oxide of all copper oxides (Figure 1a) in terms of sensing applications. It has to be underlined that  $\text{Cu}_2\text{O}$  and  $\text{Cu}_2\text{O}_3$  are not stable materials and cannot be considered as possible materials for gas-sensing applications. CuO is a typical p-type semiconductor, and it has many remarkable properties, for example: catalytic activity, optoelectronic properties, high stability, ease of access, and antibacterial activity. CuO has a large absorption of solar spectrum and thus can be used as an ideal absorption material in solar cells because its optical absorption edge ranging between 1.2 and 1.9 eV has a good match with the solar spectrum. Moreover, the investigation results have shown that CuO is stable under exposure to various gases, and relatively low changes of base resistivity were observed. It is a less expensive technology than rare materials used in gas-sensing applications [3]. Therefore, it has been utilized in various applications, including: solar energy cells [4], optoelectronics [5], catalysis [6–8], biosensors [9–13],

photoelectrochemical sensors [14,15], supercapacitors [16], lithium ion batteries [17,18], infrared photo detectors [19], electrochemical sensors [20,21], and gas sensors. Figure 1b shows the number of papers published from 1995 to now, where CuO was studied.

In this review, the latest achievements in the application of gas sensing, in which CuO thin films have been used, are presented and discussed. The paper is organized as follows: Section 2 presents various deposition techniques utilized for CuO thin film deposition and materials used to develop sensors with enhanced sensitivity/selectivity, e.g., the use of various dopants. Section 3 presents the gas sensing results under exposure to various gases and different applications, e.g., environmental pollutant detectors or healthcare monitoring. Section 4 consists of the conclusions and further perspectives for CuO thin film in gas sensors.

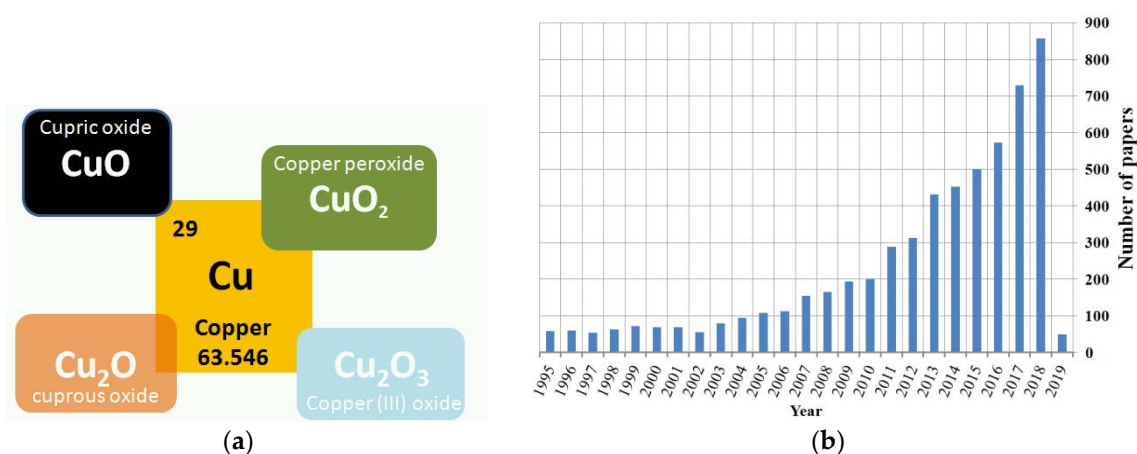


**Figure 1.** The copper oxides: (a) schematic view of the possible copper oxide forms and (b) the number of papers related to CuO-based gas sensors from 1995–2019.

## 2. Copper Oxides' Compositions and Deposition Techniques

Ideal materials for gas-sensing applications should be characterized by high 3-S parameters (sensitivity, selectivity, and stability). Other important features are fast response/recovery time(s). Since the morphology and structure of oxides play an important role in their gas-sensing characteristic, many efforts have been devoted to the development of deposition and synthesis techniques. In general, to improve the functional properties, oxides are modified by various dopants. Recently, CuO was modified by Au [22], Fe [23], Li [23,24], Na [24], Pd [25], Pt [26], Px (Piroxicam) [27], Ag [28], Cr [28], Sb [28], and Si [28]. Various techniques have been studied to deposit CuO (Figure 2), for example: magnetron sputtering [22,28–32], sol-gel [33], thermal oxidation [14,34], hydrothermal techniques [4,5,15,20,21,35–37], hydrothermal techniques with the electrospinning method [38,39], the spray pyrolysis technique [40], the microwave-assisted method [41], electron beam irradiation [42], microplasma synthesis [43], and successive ionic layer adsorption and reaction (SILAR) [44]. In [28], the author presented M-doped CuO-based thin film deposited using magnetron sputtering technology, which is a typical physical vapor deposition (PVD) technique. The sputtering process was carried out in high vacuum/ultra-high vacuum at various temperatures, including cooling and heating of the samples. It has many advantages such as easy operation, large deposition range, and low cost in large-scale production of dense and uniform films. Those features are very important for the fabrication process; moreover, magnetron sputtering can be easily adopted in lab-on-chip production or CMOS technology. It provides the possibility to fabricate the complete gas sensor device with the gas-sensitive layer and electronic circuits. Another technique used for CuO deposition is thermal oxidation, which is very similar to magnetron sputtering with the difference being that the Cu seed layer is firstly deposited and then the samples are oxidized in a furnace under a flow of pure oxygen at higher temperatures (for CuO, it is usually 400 °C). Thermal oxidation gives the possibility to obtain CuO in nanowire form, while magnetron sputtering generally creates thin films. Both techniques

require high-class equipment, which is their main disadvantage. In addition to vacuum techniques, hydrothermal processes are also used. In a typical hydrothermal synthesis of CuO, copper (II) nitrate trihydrate ( $\text{Cu}(\text{NO}_3)_2 \cdot 3\text{H}_2\text{O}$ ), sodium hydroxide (NaOH), and ethylene diamine (EDA) ( $\text{C}_2\text{H}_4(\text{NH}_2)_2$ ), as well as ethylene glycol ( $\text{C}_2\text{H}_6\text{O}_2$ ) are used. The hydrothermal methods require chemical reagents, autoclaves, furnaces, etc. However, uniformly-oriented (well distributed on the surface with a specific growth direction) structures can be obtained with this method, such as: snowflake-like, flower-like, hollow sphere-like, and urchin-like 3D [45]. The influence of water and ethylene glycol on the evolution of the morphology of the CuO nanostructures and their corresponding physical properties was studied by Bhuvaneshwari et al. [45]. The synthesized CuO superstructures were tested at room temperature under exposure to ammonia. Another method employed for the production of metal oxides such as copper oxide is a sol-gel method. There are several different synthesis routes for CuO; however, all require chemical agents (complexing and reducing), stirring and drying steps. Sol-gel methods are less expensive and easier in comparison with magnetron sputtering, which make them very attractive for fast prototyping. The main issues are the stability and repeatability of the obtained films. The method that overcomes those limitations (price and technical complications) is the spray pyrolysis technique. This technique includes essentially a nozzle ensuring deposition, a suction pump containing the desired material, and compressed gas, which controls the solution flow rate. In [40], CuO thin films were deposited on glass substrates at temperatures ranging from 300–375 °C and spraying during 20 min. Prior to deposition, substrates were cleaned with nitric acid, acetone, and distilled water to remove any dust or contaminants. The starting solution, an aqueous solution containing copper chloride  $\text{CuCl}_2$ , was used, being a source of copper, heated to a specific temperature to increase the solubility of various constituents, and then deposited on glass substrates using spray pyrolysis. Various methods allow obtaining copper oxides with different morphologies, including nanowires [44,46], nanoparticles [33,47], nanoflowers [26,48], nanofibers [38,49], nanorods [50,51], nanostructures [35,36,42], nanobelts [24], hollow spheres [8,23], and nanosheets [52]. Table 1 lists various deposition techniques and nanoscale forms of CuO-based gas sensors. Generally, the review was limited to the papers published from 2016–2018; therefore, only selected deposition techniques are shown. It has to be underlined that several other techniques such as chemical vapor deposition (CVD), atomic layer deposition (ALD), and pulse laser deposition (PLD) can be applied for CuO deposition, as well. Figure 3 shows SEM photos of various copper oxides with different morphologies.

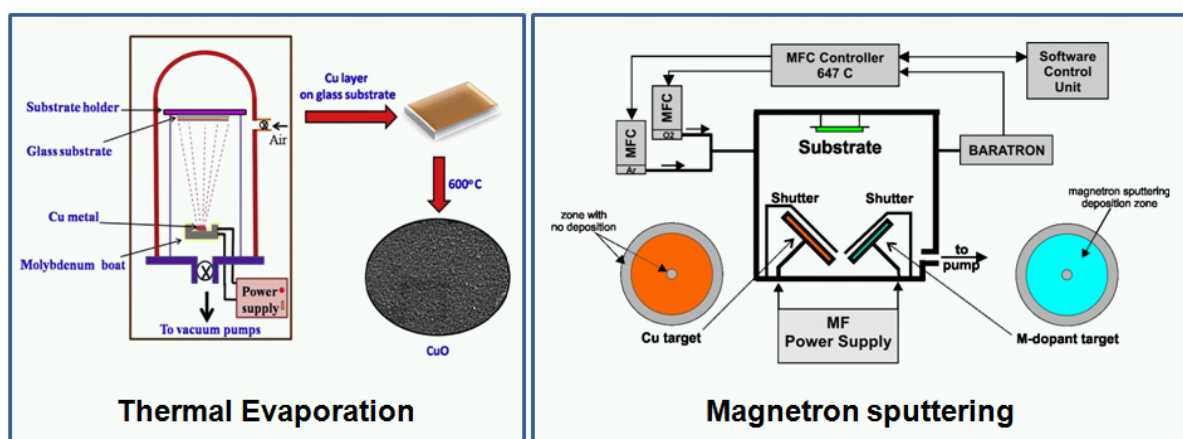


Figure 2. Cont.



**Figure 2.** The copper oxide deposition methods: (a) Thermal evaporation (Reprinted with permission from [34]); (b) Magnetron sputtering (Reprinted with permission from [28]. Copyright 2017 Elsevier); (c) Hydrothermal method (Reprinted with permission from [37]. Copyright 2017 Elsevier); (d) Facile method (Reprinted with permission from [53]. Copyright 2018 Elsevier).

**Table 1.** Selected information of various deposition techniques and nanoscale forms of CuO-based gas sensors presented in the paper.

Material	Nanoscale Form	Target Gas	Deposition Technique	Reference
CuO	nanoflowers	NH <sub>3</sub>	hydrothermal with electrospinning method	[38]
CuO	nanotubes	CO	hydrothermal	[54]
CuO	nanocubes	NO <sub>2</sub>	thermal evaporation	[55]
CuO	nanoplatelets	NO <sub>2</sub>	sonochemical method	[56]
CuO	nanoparticles	CO <sub>2</sub>	drop coating	[57]
CuO	nanostructures	Ethanol	hydrothermal	[58]
CuO	thin films	Acetone	spray pyrolysis	[40]
M-doped CuO	thin films	propane	magnetron sputtering	[28]
Cr-doped CuO	thin films	Acetone	magnetron sputtering	[59]
Cr-doped CuO	nanoboats	NH <sub>3</sub>	hydrothermal	[45]
Pd-doped CuO	nanoflowers	H <sub>2</sub> S	hydrothermal	[25]
SnO <sub>2</sub> -CuO	nanofibers	CO	electrospinning	[39]
CuO-Cu <sub>2</sub> O	nanowires	Ethanol	thermal oxidation	[60]
CuO/TiO <sub>2</sub>	nanofibers	NO <sub>2</sub> /CO	hydrothermal oxidation	[61]
CuO/rGO	nanohybrids	NO <sub>2</sub>	hydrothermal	[62]
CuO/Fe <sub>2</sub> O <sub>3</sub>	nanorods	H <sub>2</sub> S	thermal oxidation	[63]
ZnO/CuO	nanocomposite	NH <sub>3</sub>	sol-gel	[64]
CuO/CuFe <sub>2</sub> O <sub>4</sub>	microspheres	H <sub>2</sub> S	hydrothermal	[53]
Li-CuO	hollow spheres	ethanol	hydrothermal	[23]
Fe-CuO	hollow spheres	Ethanol	hydrothermal	[23]
ZnO/CuO	nanotubular	H <sub>2</sub> S	ultra-sonic pyrolysis	[65]

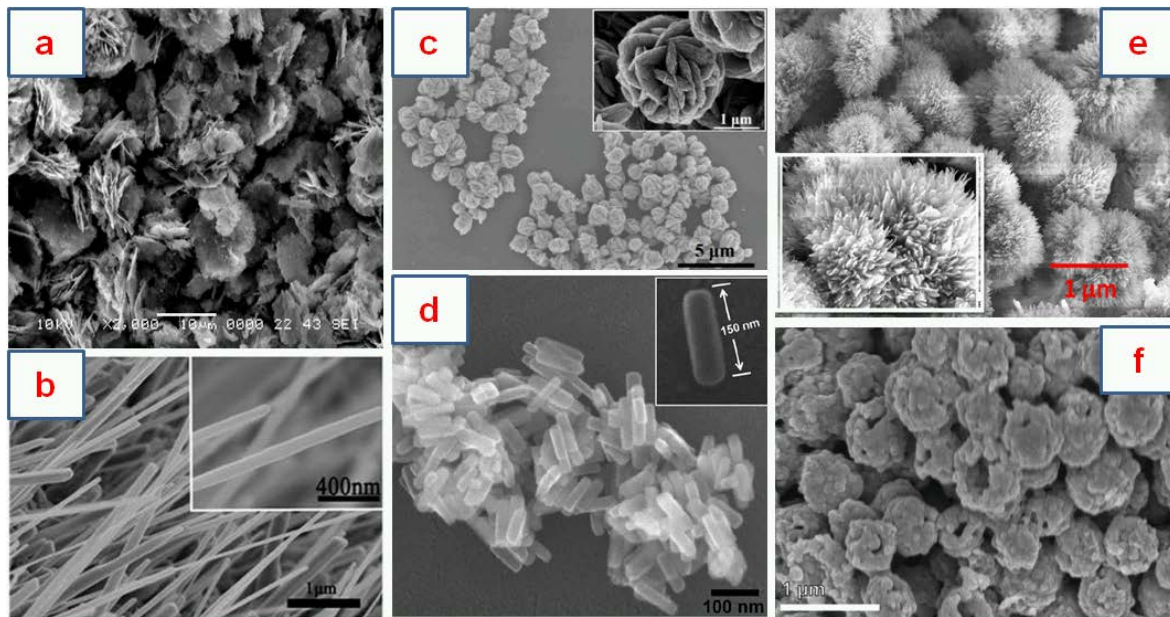


**Figure 3.** SEM photos of the copper oxides with different morphologies: (a) nanostructures (Reprinted with permission from [27]); (b) nanowires (Reprinted with permission from [16]); (c) nanostructures (Reprinted with permission from [26]); (d) nanobelts (Reprinted with permission from [24]. Copyright 2017 Elsevier); (e) nanostructures (Reprinted with permission from [45]. Copyright 2016 Elsevier); (f) hollow spheres (Reprinted with permission from [23]. Copyright 2017 Elsevier).

### 3. Results and Discussion

The number of papers presenting research findings on CuO thin film in gas sensors increased from 58 in 1995 to 857 in 2018 (108 in 2005 and 501 in 2015), which confirms that copper oxides have become attractive materials for gas-sensing applications. The gas-sensing behavior has been verified under exposure to various gases, such as: nitrogen oxides, carbon oxides, volatile organic compounds, and ammonia. The CuO-based gas sensors have been applied in various fields, including the automotive industry, environmental pollution detectors, and recently, in exhaled breath analyzers. In this section, the latest results are presented and discussed. The section is divided into subsections dedicated to different groups of target gases.

#### 3.1. Nitrogen Oxides

Nitric oxide (NO) and nitrogen oxide (NO<sub>2</sub>) are typical air pollutants that generate both smog in cities and acid rain, and they have a negative influence on human health [66]. Moreover, nitric oxide is also present in exhaled human breath and is considered to be a biomarker of several pulmonary diseases, e.g., asthma, lung cancer, or chronic obstructive pulmonary disease. Recently, Kim et al. [67] presented CuO-based gas sensors fabricated from activated carbon fibers (ACFs). The NO gas sensing behavior of the developed sensors was determined by measurements of electrical resistance, which decreased under the exposure to NO. The authors measured the untreated and treated ACF sensors. The highest results were obtained for CuO-ACFs with a 4.2 μm particle size and a 12.5% resistance change ( $((R_{NO} - R_{N_2})/R_{N_2})$ , where  $R_{NO}$  and  $R_{N_2}$  are the electrical resistances under NO and N<sub>2</sub>, respectively) for 100 ppm of NO. The authors proposed a probable mechanism of the interaction between NO gas molecules and the sensitive layer surface. The CuO particles act as catalysts to assist the movement of electrons in the ACFs. The introduction of CuO particles on the ACFs could improve the movement of electrons, as well as the NO gas detection. After injection of NO gas, NO molecules were adsorbed on the electrode surface, taking out electrons from the surface of CuO. During this process, the potential barrier decreased, and the resistance of the CuO-introduced ACFs

was lowered [67]. However, measurements were concluded only at one concentration (100 ppm) without any information concerning other conditions during the gas-sensing measurements, such as temperature and humidity. In [68], the authors developed a CuO-based gas sensor capable of selective detection of NO in a NO<sub>x</sub> mixture in a dedicated environment, which was nitric oxide detection in combustion emissions. The gas-sensitive layer was deposited on an alumina substrate with IDEs (interdigitated gold electrodes) and thermally annealed at 320 or 500 °C. The developed sensors were tested in various conditions, close to the real conditions prevailing during the operation of internal combustion engines, e.g., 300 ppm NO with increasing concentrations of NO<sub>2</sub>: 68 ppm, 113 ppm, 180 ppm, and 225 ppm. The authors carried out systematical measurements including CO interactions to gas-sensing responses. The obtained results showed that CuO exhibits greater selectivity to NO at 300 °C over NO<sub>2</sub>, and the sensor worked well in the dynamic 100–800 ppm concentration range (without sensor saturation) [68]. Navale et al. [55] presented gas sensors based on CuO nanocubes (NCs). Such sensors exhibited a maximum sensitivity  $S$  of 76% at 100 ppm NO<sub>2</sub> at 150 °C ( $S = ((R_g - R_a)/R_a) \times 100\%$ , where  $R_g$  and  $R_a$  are the electrical resistance values of CuO NCs in the presence of a target gas and air, respectively). The obtained CuO films were capable of sensing concentrations as low as 1 ppm of NO<sub>2</sub> gas [55]. Moreover, the effect of operating temperature on the NO<sub>2</sub> sensing properties of CuO films was thoroughly investigated and reported in [55]. The latest results in this field were presented by Zhao et al. [69]. Carbon nanotubes (CNTs) were prepared with CuO nanorods via the facile reflux method. The 1D composite with the molar ratio of CuO and CNTs at 2.4:1 displays excellent gas sensing performance, i.e., the lowest detectable limit of 970 ppb (parts per billion) and the short response time of 6 s at 97.0 ppm NO<sub>2</sub> at room temperature. The CuO-CNTs gas sensors are the resistance type, where the total resistance of the sensor is the sum of the resistance of 1D CuO-CNTs and the resistance between the sensitive layer and Au electrode. In the presented sensor, CNTs were behaving as a highly conductive channel and CuO as a low conductivity channel, and the total resistance largely depended on the resistance of CuO nanorods. Recently, Li et al. [62] reported the investigation results of CuO/reduced graphene oxide (CuO/rGO) nanohybrids and their responses to nitrogen oxide in the dynamic 1–75 ppm range. Upon exposure to 1 ppm NO<sub>2</sub> at room temperature, the as-prepared CuO/rGO nanohybrids showed a sensitive response of about 14 and the response time and recovery time of about 66 s and 34 s, respectively. The low detection limit was evaluated to be as low as 60 ppb at room temperature. The high response can be attributed to the large surface area of CuO/rGO nanohybrids and enhanced carrier transfer between NO<sub>2</sub> molecules and nanohybrids. The estimated ( $R^2 = 0.992$ ) sensitivity of the sensor as a function of nitrogen dioxide was  $y = 15.273 + 0.490x$ , where  $y$  is the sensitivity and  $x$  is the nitrogen dioxide concentration [62]. The investigation results on amorphous and crystalline CuO thin film under exposure to nitrogen oxides are presented in [32]. The obtained results have shown that the optimal operating temperature (100 ppm NO<sub>2</sub>, 50% RH) is lower for amorphous than for nanocrystalline CuO thin film and equals 180 °C and 325 °C, respectively. The amorphous CuO thin film exhibited faster response/recovery time (s) under the exposure to 100 ppm NO<sub>2</sub>, equal to 6 and 18 s, respectively (Figure 4a) [32]. Recently developed, nanocrystalline CuO thin films have been tested under exposure to 20 ppm NO<sub>2</sub> and at various temperatures (210, 280, 350, and 415 °C) with 50% RH [70]. Figure 4b shows the responses ( $R_{\text{air}}/R_{\text{NO}_2}$ ) and response/recovery time (s) of the deposited films. As can be noticed, the response and response/recovery time (s) decreased with temperature. The optimal conditions for such films have to be set as a compromise between higher sensitivity, fast response, and operating temperature value.

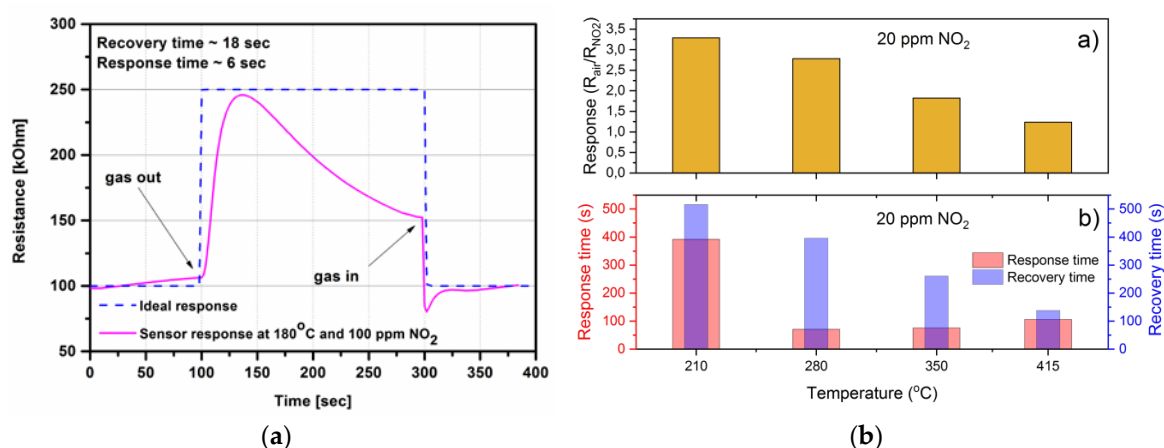


**Figure 4.** The copper oxides under exposure to nitrogen dioxide: (a) resistance change of the amorphous CuO thin film under exposure to 100 ppm of NO<sub>2</sub> at 180 °C and 50% RH (Reprinted with permission from [32]. Copyright 2014 IEEE); (b) responses and response/recovery time (s) of nanocrystalline CuO thin films under exposure to 20 ppm NO<sub>2</sub> at various temperatures and 50% RH. (Reprinted with permission from [70]. Copyright 2018 IEEE).

### 3.2. Hydrogen Sulfide (H<sub>2</sub>S)

CuO is a well-known sensor material for H<sub>2</sub>S gas detection, due to its catalytic behavior when exposed to H<sub>2</sub>S gas. The H<sub>2</sub>S detectors can be divided into two groups. The first one is focused on high concentrations of H<sub>2</sub>S, which are very dangerous for human beings [66]. The second one is developed to detect low concentrations of ppm and ppb, which is important for medical applications, such as halitosis diagnosis. Recently, Hu et al. [53] presented the gas-sensing results of H<sub>2</sub>S detection utilized by CuFe<sub>2</sub>O<sub>4</sub><sup>-</sup> and CuO-based gas sensors. The obtained results showed that the response of the optimized CuFe<sub>2</sub>O<sub>4</sub><sup>-</sup> modified heterostructures to 10 ppm H<sub>2</sub>S was approximately 20-times higher than that of pure CuO microspheres. The optimal temperature was 240 °C. The same authors in [25] presented CuO nanoflowers doped with 1.25 wt % Pd, where the optimal temperature was equal to 80 °C and the response was 123.4 to 50 ppm H<sub>2</sub>S (pure CuO exhibited 15.7). Sensors working at 50 °C were developed by Li et al. [65]. They were based on nanotubular arrays composed of hexagonal ZnO and external monoclinic CuO shells. The sensitivity ( $(R_g - R_a)/R_a \times 100\%$ ) varied in the range of 20%–45% for the dynamic 1–20 ppm H<sub>2</sub>S concentration. The sensors were prepared with two different morphologies: nanotubes and nanorods. The sensitivity in both cases was comparable; however, the response time (20 ppm H<sub>2</sub>S) was 37 s and 122 s, respectively [65]. The lowest operating temperature (40 °C) was obtained for gas sensors based on CuO doped with Pt [26]. The results indicated that the CuO sensor doped with 1.25 wt % Pt exhibited the highest response of 135 to 10 ppm H<sub>2</sub>S, which was 13.1 times higher than the response of a pure CuO sensor [26]. Recently, CuO nanowires were developed for enhanced H<sub>2</sub>S detection [71]. The authors reported a gas sensor able to detect hydrogen sulfide down to 10 ppb, even in a humid environment. Moreover, the deposition method can be employed in a CMOS backend process, enabling the realization of a fully silicon-integrated CuO nanowire gas sensing device. The operating temperature was 325 °C, and the response ( $(R_{gas} - R_{air})/R_{air}$ ) changed from 80% at 100 ppb to 160% at 500 ppb of H<sub>2</sub>S and 50% RH.

### 3.3. Carbon Oxides

Carbon oxides, i.e., carbon monoxide (CO) and carbon dioxide (CO<sub>2</sub>), have some common properties: they both are colorless and odorless gases, and at a high concentration, both can be deadly for human beings. Both gases need to be controlled for safety reasons, but in different concentration ranges. Currently, WHO recommends not extending the exposure to CO (at 760 mmHg and 20 °C) beyond 15 min for 85.8 ppm, 1 h for 30 ppm, 8 h for 8.5 ppm, and 24 h for 6 ppm [72]. Because, CO is a

colorless, non-irritant, odorless, and tasteless toxic gas, it is called “a silent killer” and kills around ~450 persons per year in the U.S. [73] and ~400 persons per year in Poland [74], and the numbers are much higher for countries with a low and middle level of development. Recently, CuO thin film gas sensors with enhanced sensitivity to CO were presented in [54]. The authors verified the CO detection for two CuO morphologies, i.e., CuO nanotubes (CuO NTs) and CuO nanocubes (CuO NCs). The obtained results demonstrated that CuO NTs exhibited a lower optimum working temperature (175 °C) and a higher sensitivity to CO in the 50–1000 ppm range. The response/recovery times were 29/37 s and 11/18 s for CuO NCs and CuO NTs, respectively (Figure 5). The structure characterization showed that the prepared CuO nanotubes and nanocubes had a rough surface and enhanced surface area, which are beneficial for gas-sensing applications [54].

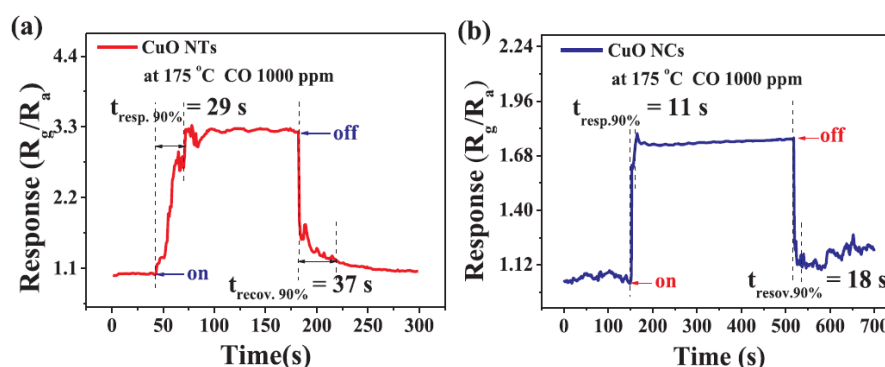


**Figure 5.** The response and recovery times of the (a) CuO NTs and (b) CuO NCs exposed to 1000 ppm. Reprinted with permission from [54]. Copyright 2018 Elsevier.

Carbon dioxide is considered to be a hazardous gas in the atmosphere, whose continuous increase in concentration can lead to adverse effects on human life and the overall environment [75]. The detection of CO<sub>2</sub> by utilization of CuO thin film gas sensors was recently presented by Tanvir et al. [57,76]. In [76], the authors presented investigation results of a gas-sensitive layer based on the combination of CuO nanoparticles with an organic binder and zinc peroxide: ZnO<sub>2</sub>. The developed layers were investigated in the 20–600 °C temperature range, at various relative humidity (RH) concentrations, such as 0%, 30%, 60%, and 80%, and in 400–4000 ppm concentration range (with 1000 ppm steps) of CO<sub>2</sub>. The highest responses were obtained at a 300 °C operating temperature and 30% RH. The obtained results showed that the CuO/ZnO<sub>2</sub>-based (10:1) gas sensor exhibited typical parameters for metal oxide-based sensors. The same group in [57] presented a CuO-based CO<sub>2</sub> detector using CuO nanoparticles. The sensors were measured under the same conditions as previously, i.e., CO<sub>2</sub> in the 400–4000 ppm range, RH concentrations: 0%, 30%, 45%, 60% and 80%; however, the operating temperature was lower, i.e., 20–110 °C. The best results were obtained at 50 °C and 45% RH. In both cases, [57] and [76], the highest responses were measured for humidified samples. It was suggested that the presence of humidity and adsorbed water is necessary to achieve the reversible reaction of CO<sub>2</sub> with the CuO sensing layer.

### 3.4. Volatile Organic Compounds

Volatile organic compounds (VOCs) are a group of chemical compounds that can evaporate easily at room temperature, and they not only pollute the environment, but also seriously affect human health [77]. Therefore, detection and monitoring of low levels of VOC concentration comprise one of the most active research fields, including the food industry, agriculture, and medical applications.

#### 3.4.1. Ethanol (C<sub>2</sub>H<sub>5</sub>OH)

Ethanol is a clear, colorless liquid that is rapidly absorbed from the gastrointestinal tract and distributed throughout the body. It has bactericidal activity and is used often as a topical disinfectant.

It is widely used as a solvent and preservative in pharmaceutical preparations, as well as serving as the primary ingredient of alcoholic beverages [78]. CuO-based sensors for ethanol detection were investigated by Umar et al. [35,58]. In 2016 [35], the authors reported a successful synthesis and characterization of the lance-shaped CuO nanostructures prepared employing the hydrothermal technique. The developed sensors were examined in the 300–450 °C temperature range under exposure to 100 ppm C<sub>2</sub>H<sub>5</sub>OH. The gas response ( $R_g/R_a$ ) was around nine at 300 °C, and this temperature was suggested to be the optimum; however, the authors did not show the responses at lower temperatures. The response/recovery times were: 65 s and 125 s, respectively [35]. In 2017 [58], the same group reported the investigation results on CuO nanosheets synthesized by the same hydrothermal method. Previously, in [35], CuO-based gas sensors were tested under the exposure to ethanol, carbon monoxide, and hydrogen, and in [79], the sensors were tested under exposure to acetone, ethanol, and methanol within the dynamic 10–200 ppm concentration range. The optimum operating temperature was increased from 300 °C [42] to 370 °C [58]; however, the response/recovery times were faster, 15/11 s respectively. The developed sensor exhibited higher response ( $R_g/R_a$ ) to ethanol (8.933) than for acetone (6.625) and methanol (5.47). The gas sensing mechanism for ultra-thin CuO nanosheets for the mentioned gases was proposed and discussed in [58]. The ethanol-sensing characteristics of CuO-based films doped with aliovalent Li(I) and Fe(III) dopants were investigated by Choi et al. [23]. Lithium and iron ions were substitutionally incorporated into the CuO lattice with the variation in lattice parameters and acted as a shallow acceptor or donor, leading to the increase or decrease of the hole density, respectively. Measurements of 1000 ppm of C<sub>2</sub>H<sub>5</sub>OH were performed at three different temperatures, 200, 300, and 400 °C, and various dopant concentrations (0–4 at % for both Li(I) and Fe(III)). The highest results were obtained at 300 °C, 1.5 at % of Fe, and was around 4.5 ( $R_g/R_a$ ); meanwhile, for 1.5 at % of Li, the response was below two. In fact, doping with Li does not improve the detection very much, i.e., the gas sensing change between pure and doped sensors is below one. The detailed results are presented in [23].

#### 3.4.2. Isopropanol (C<sub>3</sub>H<sub>8</sub>O)

Isopropanol (isopropyl alcohol or 2-propanol) is an isomer of 1-propanol. It is a colorless liquid having disinfectant properties. It is used in the manufacture of acetone and its derivatives as a solvent. Typically, it is used as an antiseptic. Small amounts of this alcohol are produced naturally by gut microbial flora [80]. The latest report about the CuO-based gas sensor to detect C<sub>3</sub>H<sub>8</sub>O was given by Zhang et al. [47]. The authors synthesized SnO<sub>2</sub> nanorods and then decorated them with CuO nanoparticles. The decoration of CuO improves the responses ( $R_a/R_g$ ) to isopropanol (100 ppm) from 22.1 for pure SnO<sub>2</sub> to 50.4 for SnO<sub>2</sub>/CuO. The optimum operating temperature was around 280 °C, and the sensors were tested under the exposure to the dynamic 20–400 ppm isopropanol range. The developed sensors exhibited fast response/recovery times equal to 4 s and 9 s, respectively. The disadvantage of the proposed n-p heterostructure was a low selectivity to other VOCs, such as: ethanol, acetone, or methanol and toluene. Figure 6a illustrates schematic diagrams of the isopropanol gas-sensing mechanism of SnO<sub>2</sub>/CuO composites. The possible energy band structure of SnO<sub>2</sub>/CuO is shown in Figure 6b. The electrons would transfer from SnO<sub>2</sub> to CuO and holes from CuO to SnO<sub>2</sub> until their Fermi levels equalize, leading to forming an additional EDL (electron-depletion layer).

In addition to the detection of isopropanol, CuO-based sensors are also used to detect n-propanol ((CH<sub>3</sub>)<sub>2</sub>CHOH). Tan et al. [81] presented CuO nanowire assembled microspheres (CuO NMs) with an extremely fast response time to n-propanol. The optimal temperature was set to 190 °C, and the response/recovery times were 1.2/6.6 s for 100 ppm and 2.7/1.2 s for 1 ppm, respectively. The sensors were tested in the dynamic range of 0–500 ppm n-propanol concentrations and a 130–260 °C temperature range. The highest response ( $R_g/R_a$ ) was obtained for n-propanol; however, the sensor had some cross-sensitivity to other VOCs, such as: methanol, ethanol, and acetone. The long-term stability test verified the possibility to use the sensor for long periods of time, which is crucial for market applications [81].

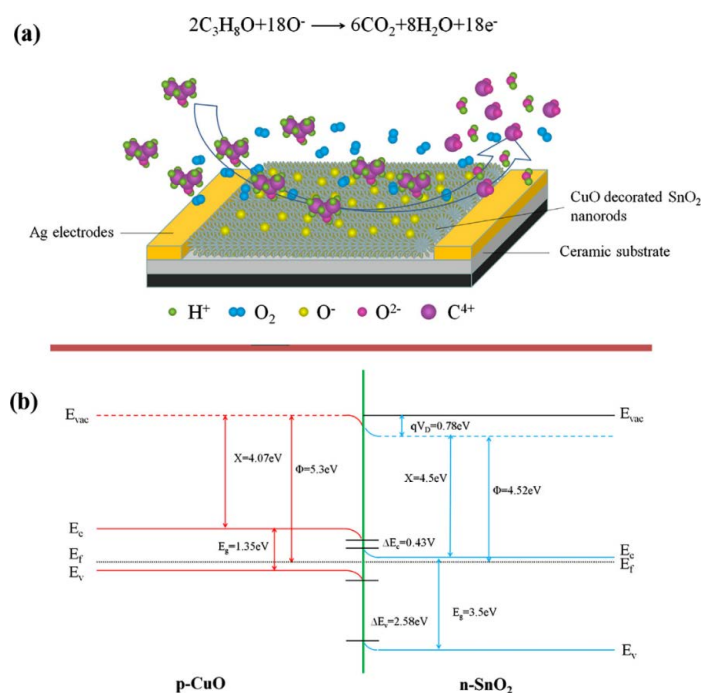


**Figure 6.** (a) Schematic view of the possible sensing mechanism of sensors based on CuO-decorated SnO<sub>2</sub> NRs and (b) the proposed energy band structure diagram of the p-CuO/n-SnO<sub>2</sub> heterojunction. Reprinted with permission from [47]. Copyright 2018 Elsevier.

### 3.4.3. Acetone (C<sub>3</sub>H<sub>6</sub>O)

Acetone is a colorless, mobile, flammable liquid readily soluble in water, ethanol, ether, etc., and itself serves as an important solvent. Acetone is an irritant, and inhalation may lead to hepatotoxic effects (causing liver damage) [82]. Except its usefulness in chemistry and industry, it has recently become more and more attractive from the medical point of view. Patients with diabetes tend to have higher acetone levels in their breath than healthy people; hence, acetone is considered as one of the biomarkers of diabetes that can be found in exhaled breath. The exhaled acetone is usually in the range of 0.2–1.8 ppm for healthy people and in the range of 1.25–2.5 ppm for people with diabetes [83]. Recently, Yang et al. [84] investigated a series of biomimetic electronic nose nanomaterials of various tungsten oxides, including WO<sub>3</sub>:CuO and pure CuO prepared by the facile method. The ability to detect acetone was verified under the exposure to 50, 100, and 200 ppm. The highest responses ( $R_g/R_a$ ) were 3.43, 5.59, and 11.9, respectively. However, the response/recovery time (s) were high: 72.2 s and 29.4 s for 50 ppm of acetone, respectively. Unfortunately, the acetone-sensing characteristics were obtained in a concentration region that is outside of interest. For medical applications, lower acetone concentrations need to be detected, and in industrial applications, generally higher (>1000 ppm) acetone concentrations occur. The conductometric acetone sensor was designed by Moumen et al. [40]. The response of CuO films in the presence of 16 ppm of acetone was investigated at a fixed temperature at 300 °C. The response (%) is defined as  $((G_{gas} - G_{air})/G_{air}) \times 100$ , where  $G_{gas}$  is the conductance in the presence of acetone and  $G_{air}$  is the conductance in air. The response change of 33% under 16 ppm was observed with very high response/recovery times: 160/360 s [40]. Recently, the acetone-sensing behavior of the Cr-doped CuO acetone sensor was published in [59]. The highest response was obtained at 450 °C (3.2 ppm of acetone) with the limit of detection at ~0.4 ppm [59]. The sensor was designed to cover the “diabetes” and “health” region, which means that it is able to detect the acetone concentrations in the range of 0.4–10 ppm. The working temperature was still high, 450 °C, and further investigations are needed to modify the CuO thin film into CuO nanostructures, which should reduce the working temperature.

#### 3.4.4. Others VOCs

In addition to the popular VOCs, such as ethanol, acetone, propanol, etc., several other VOCs have been recently detected by CuO thin film gas sensors, e.g., n-butanol ( $C_4H_{10}O$ ) [85]. It is primarily used as a solvent, as an intermediary in chemical synthesis, and as a fuel. n-Butanol is produced in small amounts by gut microbial fermentation through the butanoate metabolic pathway [85]. Yang et al. [79] synthesized the CuO polyhedrons with different amounts of  $PtO_2$  nanoparticles (0%, 2%, 3.5%, and 10%). The developed layers were exposed to n-butanol in the range of 1–10 ppm and 50–200 ppm. The highest responses ( $R_g/R_a$ ) were obtained for CuO: $PtO_2$  (3.5%), named as the S2-CuO sensor. The response/recovery time (s) for 100 ppm of n-butanol were 2.4 and 5.1 s, respectively. The long-term stability was also verified, and after 30 days, a small fluctuation was observed. The cross-sensitivity was measured for the composition of 100 ppm of n-butanol with inferring gases, i.e., ethanol, acetone, benzene, and isopropanol. The results showed that the S2-CuO composite sensor exhibited an excellent selectivity to n-butanol [79]. The response to n-butanol was recently investigated for (CuO-Cu<sub>2</sub>O)ZnO:Al heterojunctions by Hoppe et al. [86]. The developed layers with Al dopant at 0.1% were exposed to 100 ppm of n-butanol and different operating temperatures. The optimum temperature for the film was 350 °C, and it gave 200% gas response changes for n-butanol. CuO thin film gas sensors were also used to detect gases, named BTEX (benzene, toluene, ethylbenzene, and xylol). The latest results in this field have been delivered by Ren et al. [87]. The CuO/SnO<sub>2</sub> composite was synthesized and verified for its gas sensing properties under exposure to BTEX. The highest response ( $R_a/R_g$ ) of 50 ppm BTEX at 280 °C was shown for the 3 mol % CuO/SnO<sub>2</sub> composite. The pure SnO<sub>2</sub> exhibited higher sensitivity to ethanol, acetone, and ammonia, while CuO/SnO<sub>2</sub> worked 3–5 times better for BTEX in the wide concentration range of 2–200 ppm [87]. CuO thin film gas sensors have been successfully used to detect propane. Propane ( $C_3H_8$ ) is a by-product of natural gas processing and petroleum refining. It is commonly used as a fuel for engines, oxy-gas torches, barbecues, portable stoves, and residential central heating [88]. In [28], the investigation results on M-doped CuO-based (M = Ag, Au, Cr, Pd, Pt, Sb, and Si) sensors working at various temperatures upon exposure to a low concentration of propane were presented. Propane is commonly used in the chemical industry; however, it can also be found in exhaled human breath. The results showed that the addition of M-dopants in the cupric oxide film effectively acted as catalysts in propane sensors and improved their gas-sensing properties.

#### 3.5. Formaldehyde (HCHO)

Formaldehyde is a colorless, poisonous gas synthesized by the oxidation of methanol and used as an antiseptic, disinfectant, histologic fixative, and general-purpose chemical reagent for laboratory applications. Environmentally, formaldehyde may be found in the atmosphere, smoke from fires, automobile exhaust, and cigarette smoke. Small amounts are produced during normal metabolic processes in most organisms, including humans [89]. Recently, formaldehyde gas sensors based on CuO were developed by Meng et al. [37]. The sensors were exposed to formaldehyde in the 5–200 ppm range with a 300 °C optimal operating temperature. The highest responses ( $R_g/R_a$ ) were obtained for sensor synthesized at 180 °C for 12 h and resulted in four at 200 ppm. The long-term stability and selectivity measurements were carried out showing a market potential for such sensors.

#### 3.6. Ammonia (NH<sub>3</sub>)

Ammonia is a colorless, inorganic compound of nitrogen and hydrogen with the formula NH<sub>3</sub>, usually in gaseous form with a characteristic pungent odor. Ammonia is irritating to the skin, eyes, nose, throat, and lungs. It is essential for many biological processes and has various industrial applications [90]. Recently, Poloju et al. [64] investigated the possibility to utilize the Al-ZnO/CuO nanostructures for various ammonia concentration monitoring. Such structures exhibited enhanced response ( $R_a/R_g$ ) to ammonia within the 100–500 ppm range (100 ppm steps), with response/recovery

times equal to 14 and 9 s for 500 ppm, respectively. The response to  $\text{NH}_3$  was 500 times higher than for other compounds, such as: several common VOCs, gasoline, and acetylacetone [64]. Enhanced ammonia detection was obtained also by utilization of  $\text{In}_2\text{O}_3/\text{CuO}$  mesoporous structures. In [49], the various compositions of indium-copper-oxides were investigated under exposure to a wide range of dynamic ammonia concentrations: 0.3–100 ppm at room temperature. The developed layers exhibited high sensitivity  $((R_g - R_a)/R_a)$  and fast response time (s): 2 and 8 s for 100 ppm and 0.3 ppm of  $\text{NH}_3$  at room temperature, respectively. The obtained results are very promising for market applications, featuring: operation at room temperature, high sensitivity, fast response, long-term stability (verified over 30 days), and high selectivity to  $\text{NH}_3$  over  $\text{H}_2\text{S}$ ,  $\text{H}_2$ ,  $\text{CH}_4$ , and  $\text{CO}$ .

### 3.7. Relative Humidity

Water vapor is an important interfering gas in all gas-sensing application, including exhaled breath monitoring. There are several techniques to reduce the RH influence on gas measurements; however, the humidity measurements are also important in agriculture, food industry, or art (storage of works of art in a museum). Kim et al. [91] proposed a  $\text{CuO}$ -based flexible humidity sensor fabricated using a kinetic spray process. The resistance measurements showed signal sensitivity in the range of 0.16–0.18; however, the authors presented very limited information on the measurement conditions, parameters, RH ranges, etc., which makes it difficult to comment on this work [91].

### 3.8. Cross-Sensitivity Aspect in Copper Oxide-Based Gas Sensors

Sensor accuracy depends on many factors, such as temperature, humidity, age of the sensor, and the presence of interferences. Metal oxide gas sensors (including  $\text{CuO}$ ) are known to have cross-sensitivity to gases other than the target gas. In ideal conditions, the gas sensors exhibit no cross-sensitivity; however, in real conditions, cross-sensitivity will always be present. This could be a negative or a positive cross-sensitivity, decreasing or increasing the signal, respectively. The addition of dopants and optimization of the operating temperature can help to reduce the effect. Furthermore, a number of different methods have been introduced to develop selective sensor systems, such as gas separation techniques using a filter, principle component analysis, and artificial neural networks. For commercially-available sensors, the cross-sensitivity list on gases has to be provided. It has to be underlined that the negative cross-sensitivity may be riskier than the positive one, mostly in safety applications, where positive cross-sensitivity will generally indicate an alarm, while the negative one will mislead the safety system. In scientific papers, the cross-sensitivity issue is generally neglected. The authors report the experimental results on selectivity by testing gas sensors under exposure to various gases at various concentrations and widely discuss only the impact of humidity, as one of the interferences in the gas-sensing behavior. It is well known that the humidity issue is a limiting factor for commercialization and use in practical applications. Thus, it is very important to investigate the gas-sensing properties of metal oxide-based sensors in the presence of humidity, as well as their cross-sensitivity.

### 3.9. Film Structure's Influences on the Gas-Sensing Mechanism

Metal oxides are used to detect oxidizing and reducing gases in a simple and cost-effective manner. Their chemiresistive variation emanates from the oxidative or reductive interaction of the target gas with the metal oxide surface and the consequent change in the charge carrier concentration [3]. The nanoforms of gas-sensitive layers possess a large specific surface, abundant mesopores, and many oxygen defects/vacancies and chemisorbed oxygen, which could adsorb target gases. The gas-sensing properties are strongly related to the gas-sensing layer composition, e.g., the  $\text{CuO}$  nanoparticles connected with  $\text{In}_2\text{O}_3$  nanoparticles [49]; forming many junctions, such as  $\text{CuO-In}_2\text{O}_3$  (heterojunctions),  $\text{In}_2\text{O}_3\text{-In}_2\text{O}_3$ , and  $\text{CuO-CuO}$  (homojunctions), resulting in enhanced  $\text{NH}_3$  detection. Another example is the  $\text{CuO}$ -based nanocomposite prepared with CNTs (carbon nanotubes) and  $\text{CuO}$  nanorods. As was mentioned earlier (Section 3.1), such gas sensors exhibit an excellent gas sensing performance, i.e.,

the lowest detectable limit of 970 ppb of  $\text{NO}_2$  at room temperature [69]. The electronic transmission ability of CNTs is superior to that of CuO. Therefore, CNTs behaved as a highly conductive channel and CuO as a lowly conductive channel. Furthermore, due to the lack of electrons, the hole-accumulation layer served as a poor conductance channel. The high conductance channel of CNTs, combined with many low conductance channels of the CuO NRs, established the channels of electron transmission. Therefore, the resistance of 1D CuO-CNTs is largely dependent on the resistance of CuO nanorods (Figure 7a). When it was exposed to air, oxygen molecules adsorbed on the surface of the sample tended to trap the electrons from the CuO conduction band and generated  $\text{O}_2^-$  adsorbates. In the case of  $\text{NO}_2$  gas, the gas molecules could attract electrons from the gas-sensitive material because of the high electron affinity to  $\text{NO}_2$  molecules. Both processes could result in a decrease of electron density, an increase of the hole's density on the surface of the semiconductor, and a rapid decrease of the resistance of the sensor (Figure 7b) [69].

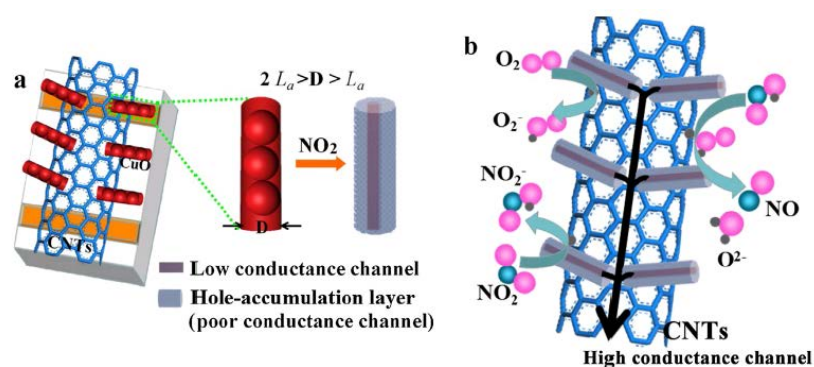


**Figure 7.** Sensing mechanism of the CuO NR-CNT composite-based sensor: (a) the model of CuO NR-CNT composite on the electrode; (b) the surface state of CuO NR in a  $\text{NO}_2$  atmosphere. Reprinted with permission from [80]. Copyright 2018 Elsevier.

In the case of gas sensors employing single or multiple nanowires between metal electrodes, the gas sensitivity can be attributed to the modulation of the carrier concentration in the nanowire channels or a Schottky barrier at the metal contact. In [71], gas-sensing properties of a CuO nanowire device were presented, where resistance changes were expected from modulation of carrier concentrations in the nanowires channels and of the potential barrier at the nanowire-nanowire contacts [71]. From the I-V characteristics presented by the authors, it can be concluded that potential barriers at grain boundaries between CuO nanowires occurred. The reaction of oxygen with an adsorption site resulted in ionosorbed oxygen species  $\text{O}^-$  and the generation of a hole, which led to an accumulation layer at the surface of the p-type conducting CuO nanowire, and thus, a decrease of resistance [71]. The film structures morphology strictly depends on the deposition techniques used for gas-sensitive layer deposition. The sensitivity, selectivity, and stability can be enhanced by combining the bare material with dopants, junctions, and different morphologies, and such methods were presented in this review for specific gas-sensing applications.

#### 4. Conclusions and Further Perspectives

The copper oxides have recently become an attractive material for gas-sensing applications, allowing one to detect several gases, such as: nitrogen oxides, carbon oxides, ammonia, hydrogen sulfide, volatile organic compounds, as well as relative humidity. The copper oxide-based sensors were utilized in various industry fields and various concentrations ranges, including high concentrations (>1000 ppm) and low concentrations (<1 ppm). However, the higher concentration for  $\text{NO}_x$  gases (>50 ppm) and  $\text{H}_2\text{S}$  gas (ppm range) is mostly too high to be interesting for real applications. The most powerful and robust manufacturing techniques for the preparation of thin films with good thickness control are vacuum-based methods. However, these methods are mostly expensive. An alternative can

be sol-gel methods, which are less expensive and easier in comparison with magnetron sputtering, making them very attractive for fast prototyping. The most important feature of the CuO thin film gas sensors is their possibility to function at low or room temperatures for a long time. Recently-published results have shown that pure CuO, as well as modified/doped CuO films can be developed by various techniques, which also increase the possibility to develop gas detectors. Table 2 shows a summary of the information presented in this review. The author of this review started his own research program to utilize CuO in the exhaled acetone measurements, as a supplementary tool for non-invasive diabetes monitoring [59,92].

**Table 2.** Summarized information of CuO-based gas sensors presented in the paper.

Material	Target Gas	Concentration (ppm)	Operating Temp. (°C)	Highest Sensitivity (%)	Reference
CuO-ACF <sup>1</sup>	NO	100	RT <sup>2</sup>	12.5	[67]
CuO	NO	300–500	300	40	[68]
CuO-TiO <sub>2</sub>	NO <sub>2</sub>	10	300	700	[61]
CuO NCs <sup>3</sup>	NO <sub>2</sub>	10–100	150	75	[55]
CuO	NO <sub>2</sub>	10–40	75	5600	[56]
CuO	NO <sub>2</sub>	100	180	3.25	[93]
CuO	NO <sub>2</sub>	20	210	3.25	[94]
CuO:NiO	NO <sub>2</sub>	1–100	RT	80	[94]
CuO CNTs	NO <sub>2</sub>	0.97–97	RT	96.4	[69]
CuO/rGO	NO <sub>2</sub>	1–75	RT	52.5	[62]
CuO/CuFe <sub>2</sub> O <sub>4</sub>	H <sub>2</sub> S	10–75	240	75	[53]
CuO:Pd	H <sub>2</sub> S	1–50	80	119	[25]
CuO:Pt	H <sub>2</sub> S	1–10	40	134	[26]
CuO NTs <sup>4</sup>	CO	50–1000	175	2.25	[54]
CuO-TiO <sub>2</sub>	CO	10	300	1400	[46]
CuO	CO	100	180	2.25	[70]
CuO NPs <sup>5</sup>	CO <sub>2</sub>	1000–4000	65	90	[54]
CuO:ZnO	CO <sub>2</sub>	400–4000	300	32.5	[57]
CuO	C <sub>2</sub> H <sub>5</sub> OH	100	300	9	[35]
CuO	C <sub>2</sub> H <sub>5</sub> OH	10–200	370	13	[58]
CuO:Li	C <sub>2</sub> H <sub>5</sub> OH	1000	300	2.5	[23]
CuO:Fe	C <sub>2</sub> H <sub>5</sub> OH	1000	300	<1	[23]
SnO <sub>2</sub> :CuO	C <sub>3</sub> H <sub>6</sub> O	10–400	280	70	[47]
CuO NWs <sup>6</sup>	C <sub>3</sub> H <sub>8</sub> O	0–500	190	7	[81]
WO <sub>3</sub> :CuO	C <sub>3</sub> H <sub>6</sub> O	200	–	1092.3	[84]
CuO:Cr	C <sub>3</sub> H <sub>6</sub> O	0.4–3.2	450	3.25	[59]
CuO:PtO <sub>2</sub>	C <sub>4</sub> H <sub>10</sub> O	1–500	180	16	[79]
(CuO-Cu <sub>2</sub> O)/ZnO:Al	C <sub>4</sub> H <sub>10</sub> O	100	350	200	[86]
CuO/SnO <sub>2</sub>	BTEX <sup>7</sup>	2–200	280	20	[87]
M <sup>8</sup> :CuO	C <sub>3</sub> H <sub>8</sub>	1	250	1.72	[28]
CuO	HCHO	5–200	180	3	[37]
Al-ZnO/CuO	NH <sub>3</sub>	100–500	RT	3000	[64]
In <sub>2</sub> O <sub>3</sub> :CuO	NH <sub>3</sub>	0.3–100	RT	1.6	[49]

<sup>1</sup> Active carbon fibers; <sup>2</sup> room temperature; <sup>3</sup> nanocubes; <sup>4</sup> nanotubes; <sup>5</sup> nanoparticles; <sup>6</sup> nanowires; <sup>7</sup> BTEX, benzene, toluene, ethylbenzene, and xylol; <sup>8</sup> M: Ag, Au, Cr, Pd, Pt, Sb, and Si.

**Funding:** The work was financially supported by the National Science Centre, Poland 2017/26/D/ST7/00355.

**Conflicts of Interest:** The author declares no conflict of interest.

## References

1. Brattain, W.H.; Bardeen, J. Surface properties of germanium. *Bell Syst. Tech. J.* **1953**, *32*, 1–41. [CrossRef]
2. Taguchi, N. Gas Detecting Device. U.S. Patent 3,695,848 A, 3 October 1972.
3. Eranna, G. *Metal Oxide Nanostructures as Gas Sensing Devices*; CRC Press: Boca Raton, FL, USA, 2011.

4. Tsai, C.-H.; Fei, P.-H.; Lin, C.-M.; Shiu, S.-L. CuO and CuO/Graphene Nanostructured Thin Films as Counter Electrodes for Pt-Free Dye-Sensitized Solar Cells. *Coatings* **2018**, *8*, 21. [[CrossRef](#)]
5. Gupta, D.; Meher, S.R.; Illyaskutty, N.; Alex, Z.C. Facile synthesis of Cu<sub>2</sub>O and CuO nanoparticles and study of their structural, optical and electronic properties. *J. Alloys Compd.* **2018**, *743*, 737–745. [[CrossRef](#)]
6. Benedetto, A.D.; Landi, G.; Lisi, L. Improved CO-PROX Performance of CuO/CeO<sub>2</sub> Catalysts by Using Nanometric Ceria as Support. *Catalyst* **2018**, *8*, 209. [[CrossRef](#)]
7. Momeni, S.; Sedaghati, F. CuO/Cu<sub>2</sub>O nanoparticles: A simple and green synthesis, characterization and their electrocatalytic performance toward formaldehyde oxidation. *Microchem. J.* **2018**, *143*, 64–71. [[CrossRef](#)]
8. Lin, L.-Y.; Karakocak, B.B.; Kavadiya, S.; Soundappan, T.; Biswas, P. A highly sensitive non-enzymatic glucose sensor based on Cu/Cu<sub>2</sub>O/CuO ternary composite hollow spheres prepared in a furnace aerosol reactor. *Sens. Actuators B Chem.* **2018**, *259*, 745–752. [[CrossRef](#)]
9. Zou, J.; Wu, S.; Liu, Y.; Sun, Y.; Cao, Y.; Hsu, J.-P.; Wee, A.T.S.; Jiang, J. An ultra-sensitive electrochemical sensor based on 2D g-C<sub>3</sub>N<sub>4</sub>/CuO nanocomposites for dopamine detection. *Carbon* **2018**, *130*, 652–663. [[CrossRef](#)]
10. Hsueh, Y.-H.; Tsai, P.-H.; Lin, K.-S. pH-Dependent Antimicrobial Properties of Copper Oxide Nanoparticles in Staphylococcus aureus. *Int. J. Mol. Sci.* **2017**, *18*, 793. [[CrossRef](#)] [[PubMed](#)]
11. Guan, P.; Li, Y.; Zhang, J.; Li, W. Non-Enzymatic Glucose Biosensor Based on CuO-Decorated CeO<sub>2</sub> Nanoparticles. *Nanomaterials* **2016**, *6*, 159. [[CrossRef](#)] [[PubMed](#)]
12. Xu, T.; Jin, W.; Wang, Z.; Cheng, H.; Huang, X.; Guo, X.; Ying, Y.; Wu, Y.; Wang, F.; Wen, Y.; et al. Electrospun CuO-Nanoparticles-Modified Polycaprolactone @Polypyrrole Fibers: An Application to Sensing Glucose in Saliva. *Nanomaterials* **2018**, *8*, 133.
13. Grigore, M.E.; Biscu, E.R.; Holban, A.M.; Gestal, M.C.; Grumezescu, A.M. Methods of Synthesis, Properties and Biomedical Applications of CuO Nanoparticles. *Pharmaceuticals* **2016**, *9*, 75. [[CrossRef](#)] [[PubMed](#)]
14. Zhan, W.; Chen, Z.; Hu, J.; Chen, X. Vertical CuO nanowires array electrodes: Visible light sensitive photoelectrochemical biosensor of ethanol detection. *Mater. Sci. Semicond. Proc.* **2018**, *85*, 90–97. [[CrossRef](#)]
15. Kwon, J.; Cho, H.; Jung, J.; Lee, H.; Hong, S.; Yeo, J.; Han, S.; Ko, S.H. ZnO/CuO/M (M = Ag, Au) Hierarchical Nanostructure by Successive Photoreduction Process for Solar Hydrogen Generation. *Nanomaterials* **2018**, *8*, 323. [[CrossRef](#)] [[PubMed](#)]
16. Zhou, L.; He, Y.; Jia, C.; Pavlinek, V.; Saha, P.; Cheng, Q. Construction of Hierarchical CuO/Cu<sub>2</sub>O@NiCo<sub>2</sub>S<sub>4</sub> Nanowire Arrays on Copper Foam for High Performance Supercapacitor Electrodes. *Nanomaterials* **2017**, *7*, 273. [[CrossRef](#)] [[PubMed](#)]
17. Zhang, J.; Wang, B.; Zhou, J.; Xia, R.; Chu, Y.; Huang, J. Preparation of Advanced CuO Nanowires/Functionalized Graphene Composite Anode Material for Lithium Ion Batteries. *Materials* **2017**, *10*, 72. [[CrossRef](#)] [[PubMed](#)]
18. So, J.-Y.; Lee, C.-H.; Kim, J.-E.; Kim, H.-J.; Jun, J.; Bae, W.-G. Hierarchically Nanostructured CuO–Cu Current Collector Fabricated by Hybrid Methods for Developed Li-Ion Batteries. *Materials* **2018**, *11*, 1018. [[CrossRef](#)] [[PubMed](#)]
19. Wang, S.B.; Hsiao, C.H.; Chang, S.J.; Lam, K.T.; Wen, K.H.; Hung, S.C.; Young, S.J.; Huang, B.R. A CuO nanowire infrared photodetector. *Sens. Actuators A Phys.* **2011**, *171*, 207–211. [[CrossRef](#)]
20. Rahman, M.M.; Alam, M.M.; Hussain, M.M.; Asiri, A.M.; Zayed, M.E.M. Hydrothermally prepared Ag<sub>2</sub>O/CuO nanomaterial for an efficient chemical sensor development for environmental remediation. *Environ. Nanotechnol. Monit. Manag.* **2018**, *10*, 1–9. [[CrossRef](#)]
21. Yuan, J.; Zhang, J.-J.; Yang, M.-P.; Meng, W.-J.; Wang, H.; Lu, J.-X. CuO Nanoparticles Supported on TiO<sub>2</sub> with High Efficiency for CO<sub>2</sub> Electrochemical Reduction to Ethanol. *Catalysts* **2018**, *8*, 171. [[CrossRef](#)]
22. Proenca, M.; Borges, J.; Rodrigues, M.S.; Domingues, R.P.; Dias, J.P.; Trigueiro, J.; Bundaleski, N.; Teodoro, O.M.N.D.; Vaz, F. Development of Au/CuO nanoplasmonic thin films for sensing applications. *Surf. Coat. Technol.* **2018**, *343*, 178–185. [[CrossRef](#)]
23. Choi, Y.-H.; Kim, D.-H.; Hong, S.-H. p-Type aliovalent Li(I) or Fe(III)-doped CuO hollow spheres self-organized by cationic complex ink printing: Structural and gas sensing characteristics. *Sens. Actuators B Chem.* **2017**, *243*, 262–270. [[CrossRef](#)]
24. Wang, R.-C.; Lin, S.-N.; Liu, J.-Y. Li/Na-doped CuO nanowires and nanobelts: Enhanced electrical properties and gas detection at room temperature. *J. Alloys Compd.* **2017**, *696*, 79–85. [[CrossRef](#)]

25. Hu, X.; Zhu, Z.; Chen, C.; Wen, T.; Zhao, X.; Xie, L. Highly sensitive H<sub>2</sub>S gas sensors based on Pd-doped CuO nanoflowers with low operating temperature. *Sens. Actuators B Chem.* **2017**, *253*, 809–817. [[CrossRef](#)]
26. Tang, Q.; Hu, X.-B.; He, M.; Xie, L.-L.; Zhu, Z.-G.; Wu, J.-Q. Effect of Platinum Doping on the Morphology and Sensing Performance for CuO-Based Gas Sensor. *Appl. Sci.* **2018**, *8*, 1091. [[CrossRef](#)]
27. Alsalmeh, A.; Arain, M.; Nafady, A.; Sirajuddin. Construction of an Ultrasensitive and Highly Selective Nitrite Sensor Using Piroxicam-Derived Copper Oxide Nanostructures. *Catalysts* **2018**, *8*, 29. [[CrossRef](#)]
28. Rydosz, A.; Szkudlarek, A. Gas Sensing Performance of M-Doped CuO-Based Thin Films Working at Different Temperatures upon Exposure to Propane. *Sensors* **2015**, *15*, 20069–20085. [[CrossRef](#)] [[PubMed](#)]
29. Al-Ghamdi, A.A.; Khedr, M.H.; Ansari, M.S.; Hasan, P.M.Z.; Abdel-Wahab, M.S.; Farghali, A.A. RF sputtered CuO thin films: Structural, optical and photo-catalytic behavior. *Phys. E Low Dimens. Syst. Nanostruct.* **2016**, *81*, 83–90. [[CrossRef](#)]
30. Du, Y.; Gao, X.; Zhang, X.; Meng, X. Characterization of the microstructure and the optical and electrical properties of the direct-current magnetron sputtered CuO films at different substrate temperatures. *Physica B Condens. Matter* **2018**, *546*, 28–32. [[CrossRef](#)]
31. Zheng, W.; Chen, Y.; Peng, X.; Zhong, K.; Lin, Y.; Huang, Z. The Phase Evolution and Physical Properties of Binary Copper Oxide Thin Films Prepared by Reactive Magnetron Sputtering. *Materials* **2018**, *11*, 1253. [[CrossRef](#)] [[PubMed](#)]
32. Rydosz, A. Amorphous and Nanocrystalline Magnetron Sputtered CuO Thin Films Deposited on Low Temperature Cofired Ceramics Substrates for Gas Sensor Applications. *IEEE Sens. J.* **2014**, *14*, 1600–1607. [[CrossRef](#)]
33. Oruc, C.; Altundal, A. Structural and dielectric properties of CuO nanoparticles. *Ceram. Int.* **2017**, *43*, 10708–10714. [[CrossRef](#)]
34. Navale, Y.H.; Navale, S.T.; Stadler, F.J.; Ramgir, N.S.; Debnath, A.K.; Gadkari, S.C.; Gupta, S.K.; Aswal, D.K.; Patil, V.B. Thermally evaporated copper oxide films: A view of annealing effect on physical and gas sensing properties. *Ceram. Int.* **2017**, *43*, 7057–7064. [[CrossRef](#)]
35. Umar, A.; Lee, J.-H.; Kumar, R.; Al-Dossary, O.; Ibrahim, A.A.; Baskoutas, S. Development of highly sensitive and selective ethanol sensor based on lance-shaped CuO nanostructures. *Mater. Des.* **2016**, *105*, 16–24. [[CrossRef](#)]
36. Baloach, Q.; Tahira, A.; Mallah, A.B.; Abro, M.I.; Uddin, S.; Willander, M.; Ibupoto, Z.H. A Robust, Enzyme-Free Glucose Sensor Based on Lysine-Assisted CuO Nanostructures. *Sensors* **2016**, *16*, 1878. [[CrossRef](#)] [[PubMed](#)]
37. Meng, D.; Liu, D.; Wang, G.; San, X.; Shen, Y.; Jin, Q.; Meng, F. CuO hollow microspheres self-assembled with nanobars: Synthesis and their sensing properties to formaldehyde. *Vacuum* **2017**, *144*, 272–280. [[CrossRef](#)]
38. Can, N. Electrospun CuO nanofibers for room temperature volatile organic compound sensing applications. *Mater. Chem. Phys.* **2018**, *213*, 6–13. [[CrossRef](#)]
39. Bai, S.; Guo, W.; Sun, J.; Li, J.; Tian, Y.; Chen, A.; Luo, R.; Li, D. Synthesis of SnO<sub>2</sub>-CuO heterojunction using electrospinning and application in detecting of CO. *Sens. Actuators B Chem.* **2016**, *226*, 96–103. [[CrossRef](#)]
40. Moumen, A.; Hartiti, B.; Comini, E.; El Khalidi, Z.; Arachchige, H.M.M.M.; Fadili, S.; Thevenin, P. Preparation and characterization of nanostructured CuO thin films using spray pyrolysis. *Superlattices Microstruct.* **2018**, in press. [[CrossRef](#)]
41. Xie, H.; Zhu, L.; Zheng, W.; Zhang, J.; Gao, F.; Wang, Y. Microwave-assisted template-free synthesis of butterfly-like CuO through Cu<sub>2</sub>Cl(OH)<sub>3</sub> precursor and the electrochemical sensing property. *Solid State Sci.* **2016**, *61*, 146–154. [[CrossRef](#)]
42. Shinde, S.K.; Kim, D.-Y.; Ghodake, G.S.; Maile, N.C.; Kadam, A.A.; Lee, D.S.; Rath, M.C.; Fulari, V.J. Morphological enhancement to CuO nanostructures by electron beam irradiation for biocompatibility and electrochemical performance. *Ultrason. Sonochem.* **2018**, *40*, 314–322. [[CrossRef](#)] [[PubMed](#)]
43. Du, C.M.; Xiao, M.D. Cu<sub>2</sub>O nanoparticles synthesis by microplasma. *Sci. Rep.* **2014**, *4*, 7339. [[CrossRef](#)] [[PubMed](#)]
44. Rafea, M.A.; Roushdy, N. Determination of the optical band gap for amorphous and nanocrystalline copper oxide thin films prepared by SILAR technique. *J. Phys. D Appl. Phys.* **2009**, *42*, 015413. [[CrossRef](#)]
45. Bhuvaneshwari, S.; Gopalakrishnan, N. Enhanced ammonia sensing characteristics of Cr doped CuO nanoboats. *J. Alloy. Compd.* **2016**, *654*, 202–208. [[CrossRef](#)]

46. Lee, J.-H.; Kim, J.-H.; Kim, S.-S. CuO–TiO<sub>2</sub> p–n core–shell nanowires: Sensing mechanism and p/n sensing-type transition. *Appl. Surf. Sci.* **2018**, *448*, 489–497. [[CrossRef](#)]
47. Zhang, B.; Fu, W.; Meng, X.; Ruan, A.; Su, P.; Yang, H. Synthesis of actinomorphic flower-like SnO<sub>2</sub> nanorods decorated with CuO nanoparticles and their improved isopropanol sensing properties. *Appl. Surf. Sci.* **2018**, *456*, 586–593. [[CrossRef](#)]
48. Yoo, R.; Yoo, S.; Lee, D.; Kim, J.; Cho, S.; Lee, W. Highly selective detection of dimethyl methylphosphonate (DMMP) using CuO nanoparticles / ZnO flowers heterojunction. *Sens. Actuators B Chem.* **2017**, *240*, 1099–1105. [[CrossRef](#)]
49. Zhou, J.; Ikram, M.; Rehman, A.U.; Wang, J.; Zhao, Y.; Kan, K.; Zhang, W.; Raziq, F.; Li, L.; Shi, K. Highly selective detection of NH<sub>3</sub> and H<sub>2</sub>S using the pristine CuO and mesoporous In<sub>2</sub>O<sub>3</sub>@CuO multijunctions nanofibers at room temperature. *Sens. Actuators B Chem.* **2018**, *255*, 1819–1830. [[CrossRef](#)]
50. Kim, K.-M.; Jeong, H.-M.; Kim, H.-R.; Choi, K.-I.; Kim, H.-J.; Lee, J.-H. Selective Detection of NO<sub>2</sub> Using Cr-Doped CuO Nanorods. *Sensors* **2012**, *12*, 8013–8025. [[CrossRef](#)] [[PubMed](#)]
51. Bertuna, A.; Faglia, G.; Ferroni, M.; Kaur, N.; Arachchige, H.M.M.M.; Sberveglieri, G.; Comini, E. Metal Oxide Nanowire Preparation and Their Integration into Chemical Sensing Devices at the SENSOR Lab in Brescia. *Sensors* **2017**, *17*, 1000. [[CrossRef](#)] [[PubMed](#)]
52. Zhang, F.; Zhu, A.; Luo, Y.; Tian, Y.; Yang, J.; Qin, Y. CuO nanosheets for sensitive and selective determination of H<sub>2</sub>S with high recovery ability. *J. Phys. Chem. C* **2010**, *114*, 19214–19219. [[CrossRef](#)]
53. Hu, X.; Zhu, Z.; Li, Z.; Xie, L.; Wu, Y.; Zheng, L. Heterostructure of CuO microspheres modified with CuFe<sub>2</sub>O<sub>4</sub> nanoparticles for highly sensitive H<sub>2</sub>S gas sensor. *Sens. Actuators B Chem.* **2018**, *264*, 139–149. [[CrossRef](#)]
54. Hou, L.; Zhang, C.; Li, L.; Du, C.; Li, X.; Kang, X.-F.; Chen, W. CO gas sensors based on p-type CuO nanotubes and CuO nanocubes: Morphology and surface structure effects on the sensing performance. *Talanta* **2018**, *188*, 41–49. [[CrossRef](#)] [[PubMed](#)]
55. Navale, Y.H.; Navale, S.T.; Galluzzi, M.; Stadler, J.; Debnath, A.K.; Ramgir, N.S.; Gadkari, S.C.; Gupta, S.K.; Aswal, D.K.; Patil, V.B. Rapid synthesis strategy of CuO nanocubes for sensitive and selective detection of NO<sub>2</sub>. *J. Alloys Compd.* **2017**, *708*, 456–463. [[CrossRef](#)]
56. Oosthuizen, D.N.; Motaung, D.E.; Swart, H.C. In depth study on the notable room-temperature NO<sub>2</sub> gas sensor based on CuO nanoplatelets prepared by sonochemical method: Comparison of various bases. *Sens. Actuators B Chem.* **2018**, *266*, 761–772. [[CrossRef](#)]
57. Tanvir, N.B.; Yurchenko, O.; Laubender, E.; Urban, G. Investigation of low temperature effects on work function based CO<sub>2</sub> gas sensing of nanoparticulate CuO films. *Sens. Actuators B Chem.* **2017**, *247*, 968–974. [[CrossRef](#)]
58. Umar, A.; Alshahrani, A.A.; Algarni, H.; Kumar, R. CuO nanosheets as potential scaffolds for gas sensing applications. *Sens. Actuators B Chem.* **2017**, *250*, 24–31. [[CrossRef](#)]
59. Szkudlarek, A.; Kollbek, K.; Klejna, S.; Rydosz, A. Electronic sensitization of CuO thin films by Cr-doping for enhanced gas sensor response at low detection limit. *Mater. Res. Express* **2018**, *5*, 126406. [[CrossRef](#)]
60. Hsu, C.-L.; Tsai, J.-Y.; Hsueh, T.-J. Ethanol gas and humidity sensors of CuO/Cu<sub>2</sub>O composite nanowires based on a Cu through-silicon via approach. *Sens. Actuators B Chem.* **2016**, *224*, 95–102. [[CrossRef](#)]
61. Deng, J.; Wang, L.; Lou, Z.; Zhang, T. Design of CuO/TiO<sub>2</sub> heterostructure nanofiber and sensing performance. *J. Mater. Chem.* **2014**, *2*, 9030–9034. [[CrossRef](#)]
62. Li, Z.; Liu, Y.; Guo, D.; Guo, J.; Su, Y. Room-temperature synthesis of CuO/reduced graphene oxide nanohybrids for high-performance NO<sub>2</sub> gas sensor. *Sens. Actuators B Chem.* **2018**, *271*, 306–310. [[CrossRef](#)]
63. Park, S.; Cai, Z.; Lee, J.; Yoon, J.I.; Chang, S.-P. Fabrication of a low concentration H<sub>2</sub>S gas sensor using CuO nanorods decorated with Fe<sub>2</sub>O<sub>3</sub> nanoparticles. *Mater. Lett.* **2016**, *181*, 231–235. [[CrossRef](#)]
64. Poloju, M.; Jayababu, N.; Reddy, R.M.V. Improved gas sensing performance of Al doped ZnO/CuO nanocomposite based ammonia gas sensor. *Mater. Sci. Eng. B* **2018**, *227*, 61–67. [[CrossRef](#)]
65. Li, D.; Qin, L.; Zhao, P.; Zhang, Y.; Liu, D.; Liu, F.; Kang, B.; Wang, Y.; Song, H.; Zhang, T.; et al. Preparation and gas sensing performances of ZnO/CuO rough nanotubular arrays for low-working temperature H<sub>2</sub>S detection. *Sens. Actuators B Chem.* **2018**, *254*, 834–841. [[CrossRef](#)]
66. Ambient (outdoor) air quality and health. Available online: [http://www.who.int/news-room/fact-sheets/detail/ambient-\(outdoor\)-air-quality-and-health](http://www.who.int/news-room/fact-sheets/detail/ambient-(outdoor)-air-quality-and-health) (accessed on 27 October 2018).

67. Kim, M.-J.; Lee, S.; Lee, K.M.; Jo, H.; Choi, S.S.; Lee, Y.-S. Effect of CuO introduced on activated carbon fibers formed by electroless plating on the NO gas sensing. *J. Ind. Eng. Chem.* **2018**, *60*, 341–347. [CrossRef]
68. Mullen, M.R.; Dutta, P.K. Building Selectivity for NO Sensing in a NO<sub>x</sub> Mixture with Sonochemically Prepared CuO Structures. *Chemosensors* **2016**, *4*, 1. [CrossRef]
69. Zhao, Y.; Ikram, M.; Zhang, J.; Kan, K.; Wu, H.; Song, W.; Li, L.; Shi, K. Outstanding gas sensing performance of CuO-CNTs nanocomposite based on asymmetrical schottky junctions. *Appl. Surf. Sci.* **2018**, *428*, 415–421. [CrossRef]
70. Rydosz, A.; Maziarz, W.; Brudnik, A.; Czapla, A.; Zakrzewska, K. CuO and CuO/TiO<sub>2-y</sub> thin-film gas sensors of H<sub>2</sub> and NO<sub>2</sub>. In Proceedings of the 2018 XV International Scientific Conference on Optoelectronic and Electronic Sensors (COE), Warsaw, Poland, 17–20 June 2018.
71. Steinhauer, S.; Brunet, E.; Maier, T.; Mutinati, G.C.; Kock, A.; Freudenberg, O.; Gspan, C.; Grogger, W.; Neuhold, A.; Resel, R. Gas sensing properties of novel CuO nanowire devices. *Sens. Actuators B Chem.* **2013**, *187*, 50–57. [CrossRef]
72. Environmental Health Criteria 213: Carbon Monoxide (Second Edition). Available online: [http://www.who.int/ipcs/publications/ehc/ehc\\_213/en/](http://www.who.int/ipcs/publications/ehc/ehc_213/en/) (accessed on 27 October 2018).
73. Sircar, K.; Clower, J.; Shin, M.K.; Bailey, C.; King, M.; Yip, F. Carbon monoxide poisoning deaths in the United States, 1999 to 2012. *Am. J. Emerg. Med.* **2015**, *33*, 1140–1445. [CrossRef] [PubMed]
74. Krzyzanowski, M.; Seroka, W.; Skotak, K.; Wojtyniak, B. Mortality and Hospital Admissions Due to Carbon Monoxide Poisoning in Poland. *BiTP* **2014**, *33*, 75–82.
75. Climate Risks from CO<sub>2</sub> and Short-Lived Climate Pollutants. Available online: <http://www.who.int/sustainable-development/housing/health-risks/climate-pollutants/en/> (accessed on 27 October 2018).
76. Tanvir, N.B.; Yurchenko, O.; Laubender, E.; Pohle, R.; Sicard, O.V.; Urban, G. Zinc peroxide combustion promoter in preparation of CuO layers for conductometric CO<sub>2</sub> sensing. *Sens. Actuators B Chem.* **2018**, *257*, 1027–1034. [CrossRef]
77. WHO Guidelines for Indoor Air Quality: Selected Pollutants; The WHO European Centre for Environment and Health, Bonn Office: Bonn, Germany, 2018.
78. HMDB0000108-Human Metabolome Database. Available online: <http://www.hmdb.ca/metabolites/HMDB0000108> (accessed on 27 October 2018).
79. Yang, B.; Liu, J.; Qin, H.; Liu, Q.; Jing, X.; Zhang, H.; Li, R.; Huang, G.; Wang, J. PtO<sub>2</sub>-nanoparticles functionalized CuO polyhedrons for n-butanol gas sensor application. *Ceram. Int.* **2018**, *44*, 10426–11043. [CrossRef]
80. HMDB0000863-Human Metabolome Database. Available online: <http://www.hmdb.ca/metabolites/HMDB0000863> (accessed on 27 October 2018).
81. Tan, J.; Dun, M.; Li, L.; Zha, J.; Li, X.; Hu, Y.; Huang, G.; Tan, W.; Huang, X. Self-template derived CuO nanowires assembled microspheres and its gas sensing properties. *Sens. Actuators B Chem.* **2017**, *252*, 1–8. [CrossRef]
82. HMDB0001659-Human Metabolome Database. Available online: <http://www.hmdb.ca/metabolites/HMDB0001659> (accessed on 27 October 2018).
83. Rydosz, A. Sensors for Enhanced Detection of Acetone as a Potential Tool for Noninvasive Diabetes Monitoring. *Sensors* **2018**, *18*, 2298. [CrossRef] [PubMed]
84. Yang, F.; Wang, F.; Guo, Z. Characteristics of binary WO<sub>3</sub>@CuO and ternary WO<sub>3</sub>@PDA@CuO based on impressive sensing acetone odor. *J. Colloid Interface Sci.* **2018**, *524*, 32–41. [CrossRef] [PubMed]
85. HMDB0004327-Human Metabolome Database. Available online: <http://www.hmdb.ca/metabolites/HMDB0004327> (accessed on 27 October 2018).
86. Hoppe, M.; Ababii, N.; Postica, V.; Lupan, O.; Polonskyi, O.; Shuett, F.; Kaps, S.; Sukhodub, L.F.; Sontea, V.; Strunskus, T.; et al. (CuO-Cu<sub>2</sub>O)/ZnO:Al heterojunctions for volatile organic compound detection. *Sens. Actuators B Chem.* **2018**, *255*, 1362–1375. [CrossRef]
87. Ren, F.; Gao, L.; Yuan, Y.; Zhang, Y.; Alqrni, A.; Al-Dossary, O.M.; Xu, J. Enhanced BTEX gas sensing performance of CuO/SnO<sub>2</sub> composite. *Sens. Actuators B Chem.* **2016**, *223*, 914–920. [CrossRef]
88. HMDB0031630-Human Metabolome Database. Available online: <http://www.hmdb.ca/metabolites/HMDB0031630> (accessed on 27 October 2018).
89. NCI Thesaurus. Available online: [https://ncit.nci.nih.gov/ncitbrowser/ConceptReport.jsp?dictionary=NCI\\_Thesaurus&ns=NCI\\_Thesaurus&code=C29744](https://ncit.nci.nih.gov/ncitbrowser/ConceptReport.jsp?dictionary=NCI_Thesaurus&ns=NCI_Thesaurus&code=C29744) (accessed on 27 October 2018).

90. NCI Thesaurus. Available online: [https://ncit.nci.nih.gov/ncitbrowser/ConceptReport.jsp?dictionary=NCI\\_Thesaurus&ns=NCI\\_Thesaurus&code=C76698](https://ncit.nci.nih.gov/ncitbrowser/ConceptReport.jsp?dictionary=NCI_Thesaurus&ns=NCI_Thesaurus&code=C76698) (accessed on 27 October 2018).
91. Kim, H.; Park, S.; Park, Y.; Choi, D.; Yoo, B.; Lee, C.S. Fabrication of a semi-transparent flexible humidity sensor using kinetically sprayed cupric oxide film. *Sens. Actuators B Chem.* **2018**, in press. [[CrossRef](#)]
92. Rydosz, A.; Szkudlarek, A.; Ziabka, M.; Domanski, K.; Maziarz, W.; Pisarkiewicz, T. Performance of Si-doped WO<sub>3</sub> thin films for acetone sensing prepared by glancing angle DC magnetron sputtering. *IEEE Sens. J.* **2016**, *16*, 1004–1012. [[CrossRef](#)]
93. Selene, C.H.; Chou, J. Hydrogen Sulfide: Human Health Aspects. *Concise Int. Chem. Assess. Doc.* **2003**, *53*, 7–14.
94. Dufbartey, G.J. H<sub>2</sub>S as a possible therapeutic alternative for the treatment of hypertensive kidney injury. *Nitric Oxide* **2017**, *64*, 52–60. [[CrossRef](#)] [[PubMed](#)]



© 2018 by the author. Licensee MDPI, Basel, Switzerland. This article is an open access article distributed under the terms and conditions of the Creative Commons Attribution (CC BY) license (<http://creativecommons.org/licenses/by/4.0/>).